JOURNAL OF CATALYSIS 108, 1–14 (1987)

Properties of Boron-Substituted ZSM-5 and ZSM-11 Zeolites

G. COUDURIER,* A. AUROUX,* J. C. VEDRINE,*,[1] R. D. FARLEE,† L. ABRAMS,† AND R. D. SHANNON†

*Institut de Recherches sur la Catalyse (CNRS), 2 Avenue Albert Einstein, 69626 Villeurbanne Cedex, France; and †Central Research and Development Department, Experimental Station, E. I. du Pont de Nemours & Company, Wilmington, Delaware 19898[2]

Received August 5, 1986; revised March 31, 1987

Using NMR and IR spectroscopy boron-substituted pentasil zeolites are found to contain four-coordinated B in the hydrated state and three-coordinated B in the dehydrated state. In addition a new tetrahedral B site assigned to $(HO)_2B(H_2O)(OSi)$ was characterized by its NMR quadrupole coupling constant and asymmetry parameter. Ammonia adsorption microcalorimetry gave heats of adsorption of ~65 kJ/mol for H–B–ZSM-11 and showed that B-substituted pentasils have only very weak acidity. Calcination at 800°C increased the heat of NH_3 adsorption to ~170 kJ/mol by creation of strong Lewis acid sites. The lack of strong Brønsted acid sites in H–B–ZSM-11 was confirmed by poor catalytic activity in methanol conversion and in toluene alkylation with methanol.

INTRODUCTION

The zeolites ZSM-5 and ZSM-11 belong to the high silica "pentasil" family with a network of channels having approximate diameters of 0.51–0.55 nm. The channels are straight in ZSM-11 and straight and sinusoidal in ZSM-5 (*1*, *2*). Strong acid sites in the interior of the channels of ZSM-5 and ZSM-11 allow these zeolites to exhibit catalytic shape selectivity (*3*) in the conversion of methanol or ethanol to hydrocarbons (*4*) or in the alkylation of toluene by methanol (*5*, *6*).

The substitution of Al by B during the synthesis of pentasil zeolites has been demonstrated by a variety of investigators (*7*–*16*). This substitution might be expected to modify the acidic properties of the zeolite and thereby the catalytic properties (*7*, *9*, *10*, *17*). In this paper, in order to evaluate the differences between B and Al pentasil-type zeolites we have compared sorption capacities, IR spectra, acidities, and methanol alkylation behavior of H–B,Al–ZSM-5, and H–B–ZSM-11 with the corresponding Al forms of ZSM-5 and -11. Characterization was accomplished by chemical analysis, infrared spectroscopy, electron microscopy, X-ray diffraction, sorption, NH_3 microcalorimetry, and ^{11}B MAS NMR spectroscopy.

[1] To whom correspondence should be addressed.

[2] Contribution #4366.

EXPERIMENTAL

Starting materials for ZSM-5 were Ludox LS-30, sodium aluminate, NaOH, and tetrapropylammonium (TPA) bromide. Preparation of ZSM-5 was made following the method described by Rollman and Valyocsik (*18*). Typical samples were prepared by combining solutions containing Ludox and TPA Br and adding to this a solution of NaOH and Na aluminate. This was placed in a Hastelloy or titanium autoclave and heated at 160°C for 24 h.

Starting materials for ZSM-11 were NaOH, sodium aluminate, Ludox LS-30, and tetrabutylphosphonium chloride or tetrabutylammonium iodide as the template. Procedures described by Chu (*19*) were used to prepare ZSM-11.

B–ZSM-11 was prepared according to example 20 of Ref. (*20*) using tetrabutylammonium hydroxide, boric acid, tetraethyl-

0021-9517/87 $3.00

orthosilicate (TEOS), and KOH. B,Al–ZSM-5 was prepared according to a modification of example 15 of Ref. (*20*) using 37.5 g H_3BO_3, 133.1 g TPA Br (50% solution), 124.8 g TEOS, and 18.2 cm^3 NH_4OH. The sample was heated at 165°C for 5 days. After reaction, the products were filtered, washed with water, and heated to 500°C in air to decompose the alkylammonium ion. The H^+ forms were prepared by exchange with 10% NH_4NO_3 four times at 80°C and deammoniation at 540°C in flowing N_2. This procedure resulted in a 10- to 20-fold reduction in the Na content, giving typically 200 ppm to 0.2 wt% Na.

X-ray diffraction patterns were obtained on samples equilibrated over saturated NH_4Cl solutions using a Guinier–Hägg focusing camera (r = 40 mm). The radiation was monochromatic Cu$K\alpha$1 (λ = 0.154051 nm). KCl (a = 0.62931 nm) was used as an internal standard. Line positions on the film were determined to ±5 μm with a David Mann film reader. Cell dimensions were obtained by least-squares refinement.

Analysis of Na and Al content was made using atomic absorption, whereas B analysis was performed using the inductive coupled plasma technique. H_2O content was determined from weight loss at 1000°C and SiO_2 was determined by difference.

Adsorption was measured gravimetrically using an apparatus similar to that described by Landolt (*21*). After the samples were weighed, they were mounted onto the sorption manifold and exposed to vapor at 0.1–0.5 of the vapor pressure of the sorbate at the temperature of the samples. The amount sorbed at 20 h was used for comparison purposes. The precision of this technique is ±0.5 mg/g of sample. All sorbates were vacuum distilled, subjected to several freeze–pump–thaw cycles, and stored over a dry zeolite 4A sieve in a bulb with a vacuum stopcock.

A sample of Cab-O-Sil fumed silica, grade MS-7, with an external surface area of 200 m^2/g was used as a reference. Under the sorption conditions, the amount of sorbate pickup by the Cab-O-Sil was used to determine k, the surface coverage of sorbate expressed as a sorbate per square nanometer.

IR spectra were recorded at 25°C with a Perkin–Elmer 580 spectrophotometer with a resolution of 2.5 to 3.7 cm^{-1}. For lattice vibrational mode studies, KBr pellets were used with a 0.25% dilution. For studies of the hydroxyl groups and of NH_3 adsorption, the samples were compressed into 2 to 5 mg · cm^{-2} self-supported wafers using 2 × 10^6 Pa pressure. The samples were progressively evacuated up to 400 or 800°C and then small increments of NH_3 (0.15 NH_3/u.c.) were adsorbed up to saturation. Desorption of NH_3 was performed by progressively heating in stages of 2 h at increasing temperatures.

Both toluene alkylation with methanol at 400°C and methanol conversion reactions at 370°C were studied using a flow microreactor on line with two gas chromatographs. The samples (~50 mg) were activated under N_2 at atmospheric pressure at 400°C for 14 h. In the case of toluene alkylation, a mixed feed with N_2 as a gas carrier and with a molar methanol : toluene ratio of ca. 1 : 4 and WHSV equal to 5 h^{-1} was admitted to the catalyst. For the methanol conversion reaction, the space velocity was WHSV = 10 h^{-1} and the reaction temperature was 370°C.

^{11}B spectra were obtained at 96.3 MHz (7-T magnetic field) using a Bruker CXP-300 spectrometer. Spectra were obtained using 30° (1.5-μs) pulses and a 0.5-s recycle delay, without proton decoupling. The small pulse angle is necessary if quantitative spectra are to be obtained for sites with different quadrupole coupling constants. Typically, 1000 scans were averaged. Spectra were recorded with magic-angle spinning (MAS) at ca. 4.5 kHz and of stationary samples to fully separate and identify the boron sites. Chemical shifts are referenced to external $BF_3 \cdot Et_2O$ using 1 M H_3BO_3 in H_2O as a secondary standard (+19.2 ppm).

Relative areas of the observed boron

TABLE 1

Chemical Compositions of B and Al Forms of ZSM-5 and ZSM-11

Sample	Composition[a]/u.c.	Si/*M*
H–B,Al–ZSM-5	$H_{2.2}B_{1.8}Al_{0.4}Si_{93.8}O_{192}27, 5H_2O$	42.6
H–Al–ZSM-5	$H_{1.7}Na_{0.3}Al_{2.0}Si_{94.0}O_{192}$	47.0
H–B–ZSM-11	$H_{1.3}B_{1.3}Si_{94.7}O_{192}25, 6H_2O$	72.8
H–Al–ZSM-11	$H_{2.8}Na_{0.1}Al_{2.9}Si_{93.1}O_{192}22, 4H_2O$	32.1
H–Al–ZSM-11	$H_{1.2}Na_{0.1}Al_{1.3}Si_{94.7}O_{192}18, 4H_2O$	72.8

[a] Si + Al was taken to be 96; proton content was calculated as the difference between the B + Al and the Na contents.

resonances were obtained using the cut-and-weigh method, or by nonlinear least-squares fitting to the theoretical powder pattern lineshapes. Although the quadrupole coupling constant of the tetrahedral sites is small (<0.5 MHz), the slight asymmetry of the lineshape and narrowing by a factor of 4 produced by MAS suggest that it is still the dominant source of line broadening. Therefore, the central transition observed with MAS should contain negligible intensity from the satellite transitions, and integrated areas of the resonances are taken to be directly proportional to their relative concentrations.

Heats of adsorption of ammonia were measured in a Setaram Tian-Calvet high-temperature microcalorimeter maintained at 148°C. The volumetric system previously described (*22*) was modified to allow continuous pressure measurement using a Datametrics Barocel gauge.

Samples approximately 100 mg in weight were evacuated at a temperature of 400 or 800°C for 16 h. Adsorption experiments were carried out using NH_3 dried and deoxygenated over Na spaghetti and further purified by freeze–pump–thaw cycles over dehydrated zeolite Y.

RESULTS AND DISCUSSION

A. Chemical Analysis, Electron Microscopy, X-Ray Diffraction, and Sorption

Tables 1 and 2 show the chemical compositions, crystallite sizes, and sorption characteristics of the B– and Al–ZSM-5 samples, and their ZSM-11 counterparts.

Transmission and scanning electron micrographs of the two boralite samples showed the crystals to have different morphologies. The B,Al–ZSM-5 crystallites took the form of flat platelets of the Z-1 type bounded by (100) and (010) planes as already described (*23–27*). The B–ZSM-11 crystallites had the appearance of bundles of 90° intergrown plates (see Fig. 1).

The X-ray diffraction patterns of the ZSM-11 sample contained lines at 0.381 and 0.365 nm and the 1.00-nm line appeared to be split. Neither the 0.381- and 0.361-nm lines nor the splitting can be accounted for by the tetragonal cell reported by Kokotailo *et al.* (*2*).

Reduction of unit cell dimensions because of the smaller size of B^{3+} (0.011 nm) relative to Al^{3+} (0.039 nm) (*28*) is one of the strongest arguments for the belief that the B is located substitutionally in the lattice rather than in the channels. The cell dimen-

TABLE 2

Physical Properties of B and Al Forms of ZSM-5 and ZSM-11

Sample	Crystallite size (μm)	Cell dimensions (Å)			*V* (Å^3)	Percentage sorbed in 20 h			
		a	b	c		*n*-hex	3MeP	CCl_4	2,2DMB
H–B,Al–ZSM-5	0.2–1.5	19.884 (5)	19.780 (5)	13.300 (3)	5231	11.5	8.2	12.4	1.4
H–Al–ZSM-5	2–4	20.135 (4)	19.947 (8)	13.458 (5)	5405	13.1	10.0	13.5	1.7
H–B–ZSM-11	0.2–0.3	19.906 (6)		13.359 (3)	5293	12.9	10.0	16.3	3.9
H–Al–ZSM-11	0.3–1	20.03 (2)[a]		13.44 (2)[a]	5392	13.2	10.5	16.1	6.1
H–Al–ZSM-11	3–6	20.08 (1)		13.46 (1)	5427				

[a] Approximate values only because of reflections which violate tetragonal symmetry.

sions of B-substituted samples are significantly smaller than those of the Al-substituted samples. This is in agreement with the results of other investigators. Although our unit cell dimensions were determined in a manner similar to that of Meyers *et al.* (*29*), they agree only approximately on an absolute or relative scale. Our Al–ZSM-5 with 2.0 Al/u.c. has a unit cell volume of 5.405 nm^3 compared to an interpolated value of 5.37 nm^3 found by Meyers *et al.* (*29*). Similarly a B content of 1.3/u.c. was found to reduce our unit cell volume of ZSM-11 by 2.5% whereas 1.7 B/u.c. reduced the unit cell volume of ZSM-5 of Meyers *et al.* by 0.7%.

In the last columns of Table 2 sorption capacities of the boralites are compared with those of ZSM-5 and ZSM-11. Although H–Al–ZSM-11 and H–Al–ZSM-5 sorb similar quantities of smaller molecules like *n*-hexane and 3-methylpentane, H–Al–ZSM-11 adsorbs significantly greater quantities of the larger molecules such as cyclohexane, *o*-xylene, and 2,2-dimethylbutane. Note that H–B,Al–ZSM-5 and H–B–ZSM-11 sorbed only slightly less of the smaller molecules than the Al forms. This shows that differences in void volume due to boron incorporation in the lattice are very small; this agrees with the slight changes noted in unit cell volumes. In contrast, differences between ZSM-5 and ZSM-11 are more significant; this is perhaps due to larger channel intersections in ZSM-11.

B. NMR Data

NMR spectra of quadrupolar nuclei such as ^{11}B (spin $\frac{3}{2}$) consist of the superposition of central and satellite transitions. The satellite transitions (e.g., $\pm\frac{1}{2}$ to $\pm\frac{3}{2}$) are shifted to first order in the quadrupole interaction. In powders, this results in a powder pattern lineshape (*30*) whose width is of the order of the quadrupole coupling constant (ca. 2.5 MHz for trigonal boron sites). The large width of these transitions makes them difficult to observe or to quantify. However, the central transition ($\frac{1}{2}$ to $-\frac{1}{2}$) is shifted only to second order in the quadrupole interaction and has a width of the order of the quadrupole coupling constant squared divided by the Larmor frequency. This

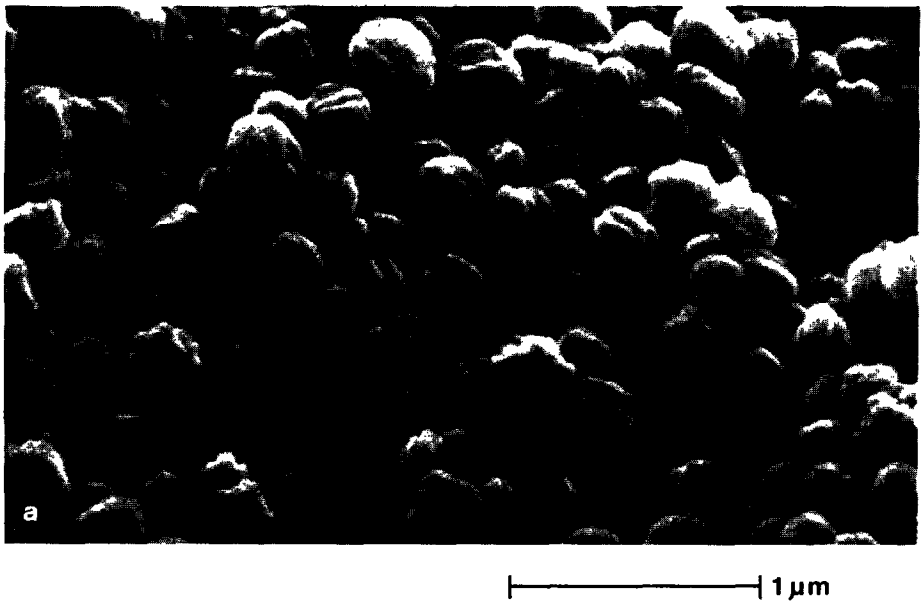

FIG. 1. Scanning electron (a) and transmission electron micrographs (b) of B–ZSM-11.

FIG. 1—*Continued.*

transition becomes narrower at higher magnetic fields and is readily observed. Its lineshape contains information on the magnitude and symmetry of the electric field gradient at the nucleus, which is produced primarily by bonding electrons centered on

the nucleus observed. The lineshape is thus a very sensitive probe of the local structure and electronic environment.

Magic-angle spinning (MAS) removes broadening arising from dipolar couplings, first-order quadrupole interactions (*31*), and chemical-shift anisotropy. The second-order quadrupole interaction is modified, but not removed, by spinning (*32*). Vega (*33*) and Kundla *et al.* (*34*) have independently derived the second-order quadrupole lineshape of the central transition produced by MAS, and it has been observed experimentally for a number of nuclei (*35*). Although MAS narrows the quadrupole splitting of the MAS lineshape by a factor of ca. 4, the singularities are typically easier to observe accurately because of the improved resolution. Variable-angle spinning (*35*, *36*) sacrifices resolution and offers no discernible advantages when the number of inequivalent sites to be resolved from one another is not large.

Bray and co-workers have used nonspinning ^{11}B NMR to study the structure of B_2O_3 (*37*) and of various borate glasses (*38*, *39*). They distinguish trigonal and tetrahedral boron by a large difference in their quadrupole coupling constants, observed to be 2.6 to 2.9 MHz and <0.5 MHz, respectively. Further, they are able to identify neutral BO_3 sites (with three bridging oxygens) from negatively charged BO_3 sites (two bridging, one nonbridging oxygen) by their asymmetry parameters, ca. 0.1 and 0.6, respectively. Because of the low frequency at which Bray worked (8–16 MHz), chemical-shift differences were not observed.

^{11}B spectra of several borosilicate minerals have also been obtained with MAS (*40*).

Scholle and Veeman (*16*) have reported ^{11}B spectra of one sample of H-boralite (Si/B = 75) in which trigonal boron was produced upon dehydration and could be completely and reversibly converted back to tetrahedral boron by rehydration. This was ascribed to the breaking of an Si–O–B bridge to form a planar, trigonal BO_3 site adjacent to an acidic SiOH in the frame work.

Several other workers have taken the observation of tetrahedral ^{11}B NMR signal as evidence for the incorporation of boron into the ZSM-5 framework (*15*, *41*, *42*).

In our samples of B–ZSM-11 and B,Al–ZSM-5 with various degrees of hydration, three different boron sites are observed by ^{11}B NMR. Because of their differences in quadrupole coupling constants, these sites are more readily separated in nonspinning than in MAS spectra. Their NMR parameters are summarized in Table 3.

In fully or partially hydrated samples, boron is predominantly in site 1, assigned as tetrahedral $B(OSi)_4$. This is readily seen as a narrow, symmetrical line with no resolvable second-order quadrupole structure.

Site 2 is also observed in fully and partially hydrated samples. The areas of the resonances associated with the various sites are listed in Table 4. The assignment of site 2 is discussed below.

In dehydrated samples, essentially all of the boron is converted to trigonal site 3 as observed by Scholle and Veeman (*16*). The central transition has a width of 3.2 kHz, so fast MAS (5 kHz) can separate and minimize the intensity of the sidebands. As reported in Table 4, a very small amount of tetrahedral site 1 remains, even in fully dehydrated samples.

While sites 1 and 3 have been observed in a variety of materials as discussed above, site 2 has not been previously reported (see Fig. 2). The quadrupole coupling constant of site 2 is very different from that reported

TABLE 3

^{11}B NMR Parameters of the B Sites

Site	Isotropic chemical shift (ppm)	Quadrupole coupling constant (MHz)	Quadrupole asymmetry parameter
1	−4	<0.5	–
2	+22	−1.9	1.0
3	+25	+2.4	0.0

TABLE 4

Areas of the ^{11}B Resonances

Sample	Site 1	Site 2	Site 3
	Hydrated[a]		
H–B–ZSM-11	0.72	0.28	0.00
H–B,Al–ZSM-5	0.69	0.31	0.00
	Partially hydrated[b]		
H–B–ZSM-11	0.65	0.35	0.00
H–B–ZSM-11, 800°C	0.47	0.53	0.00
H–B,Al–ZSM-5	0.44	0.56	0.00
	Dehydrated[c]		
H–B–ZSM-11	0.03	0.00	0.97
H–B,Al–ZSM-11	0.02	0.00	0.98

[a] Exposed to saturated NH_4Cl solution, 25°C, 24 h.
[b] Exposed to atmospheric air, 25°C, >100 h.
[c] 280°C, vacuum, 40 h.

in the literature for any trigonal site, so site 2 must be four-coordinate. The asymmetry parameter, 1.0, indicates substantial bond-angle distortion (local C_{2v}, not C_{3v}, symmetry about boron).

There are two sites in known structures which have quadrupole asymmetry parameters of 1.0 and coupling constants comparable in magnitude to that of site 2. The distorted tetrahedral $B(OB)_3(OH)$ site in $Na_2B_4O_7 \cdot 10H_2O$ (borax) has a quadrupole coupling constant of +1.63 MHz (*43*). Jellison and Bray (*44*) observed a site in sodium borate glasses with a quadrupole coupling constant of 0.72 MHz and assigned it to a distorted tetrahedral site bonded to both BO_3 and BO_4 groups, probably in a diborate unit.

This leads to the conclusion that site 2 is a highly distorted four-coordinate site, probably a framework defect such as $HOB(OSi)_3$, $(HO)_2B(OSi)_2$, or $(HO)_2B(H_2O)(OSi)$. As it is seen at comparable levels in samples with and without Al, it is unrelated to the presence of Al in the framework. The high levels of site 2 observed in the partially hydrated samples rule out the possibility of site 2 being associated with an amorphous or other second phase. The amount of site 2 is increased after calcination at 800°C and rehydration, consistent with its assignment as a framework defect. However, the NMR data alone do not allow a firm conclusion about the detailed structure of this site.

C. Microcalorimetry

Figure 3 shows plots of Q vs the quantity of NH_3 adsorbed (θ) for H–Al–ZSM-11 and H–B–ZSM-11. The heats of adsorption at low NH_3 coverage for H–ZSM-11 are higher than those published earlier by Auroux *et al.* (*45*). Strong acid sites adsorb the first doses of NH_3 up to 1.8 NH_3/u.c. which is 65% of the total OH concentration found from chemical analysis. Heating the sample to 800°C under vacuum to remove OH increases the strength of the strongest sites from 150–160 to 175–185 kJ mol^{-1} but in contrast to other samples of ZSM-5 (*46*) does not seem to reduce the total number of acid sites.

It has been observed that when the NH_3 increments introduced in the samples are very small and/or when adsorption time is long enough, no maximum is obtained in the Q–θ plot. This clearly shows that diffusion of NH_3 molecules is limited within the channels due to chemical interaction with acid sites.

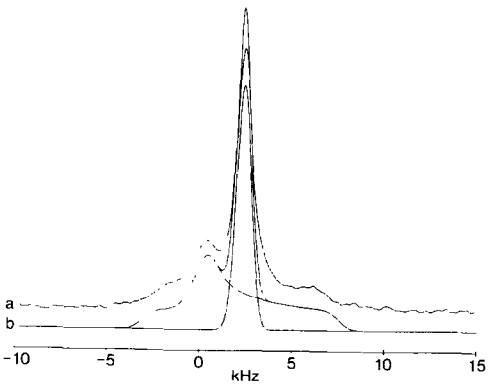

FIG. 2. ^{11}B NMR spectrum of partially hydrated H–B,Al–ZSM-5 obtained without magic-angle spinning (stationary sample): (a) experimental spectrum (11,500 scans using conditions specified in the text); (b) deconvolution showing the separate resonances arising from site 1 (1.1 kHz FWHH Gaussian), site 2 (quadrupole powder pattern corresponding to the parameters listed in Table 3, and with 1.25 kHz FWHH Gaussian broadening), and their sum. All parameters are determined by nonlinear least-squares fitting to the experimental spectrum.

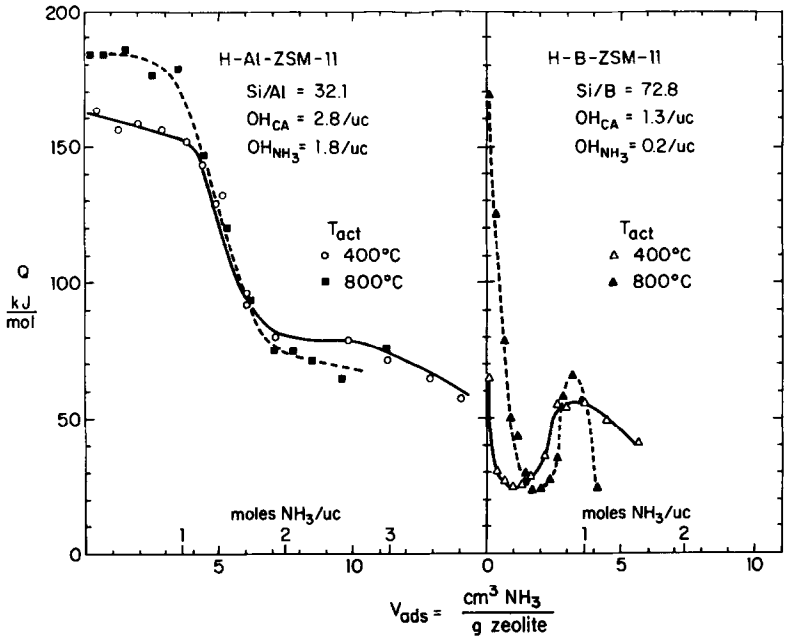

FIG. 3. Differential heats of ammonia adsorption on H–Al–ZSM-11 at 148°C.

H–B–ZSM-11 has only very weak acid sites (~65 kJ/mol) and only very few of these, viz. 0.2 NH_3/u.c. compared to 1.3 OH/u.c. by chemical analysis. The heats of adsorption rapidly diminish to 25 kJ mol^{-1} then increase to about 60 kJ mol^{-1} before decreasing again. This maximum in the Q vs θ plot seems to be related to the presence of boron. Such an additional maximum might be attributed to the formation of a $NH_4(NH_3)_n^+$complex formed by reacting B–OH–NH_3 with NH_3 ligands, similar to the gas phase $M(NH_3)_n^+$ clusters found by Castleman *et al.* (*48*).

Dehydroxylating H–B–ZSM-11 at 800°C dramatically increases the strength of the acid sites to 170 kJ mol^{-1} and sharpens the maximum at 0.8 NH_3/u.c. We propose that a few strong Lewis acid sites are formed upon dehydroxylation. This is consistent with the relative Lewis acid strengths of B and Al found by Zhang (*47*).

In Fig. 4 H–Al–ZSM-5 is seen to behave somewhat differently from other samples of H–ZSM-5 previously investigated. Instead of showing a maximum in the Q–θ plot, there is a continuous and sharp drop in acid strengths from 178 to 110 kJ mol^{-1} as NH_3 is added from θ = 0 to 1.2 NH_3/u.c. As in H–ZSM-11 there is a plateau at ~70–80 kJ mol^{-1}. Strong acid sites are available up to 1.2 NH_3/u.c. compared to 1.6 OH/u.c. by chemical analysis.

H–B,Al–ZSM-5 behaves similarly to a H–Al–ZSM-5 sample with a low Al concentration. The effect of B in this sample is masked by the Al but a maximum in the Q vs θ plot was observed as for the H–B–ZSM-11 sample.

D. IR Data

a. Mid-infrared spectra. The mid-infrared spectra of all samples (Fig. 5) are characteristic of the pentasil family (*49*, *50*) with absorption bands near 1230, 1100, 800, 560, and 455 cm^{-1} and optical density ratios of the 560- to 455-cm^{-1} bands equal to ca. 0.6 as usually observed for pentasil zeolites (*49*). The frequency of the 1100-cm^{-1} band decreased from 1102 cm^{-1} for H–B–ZSM-11 to 1098 cm^{-1} for H–Al–ZSM-11 with the Si/M ratio decreasing from 72.8 to 15.6.

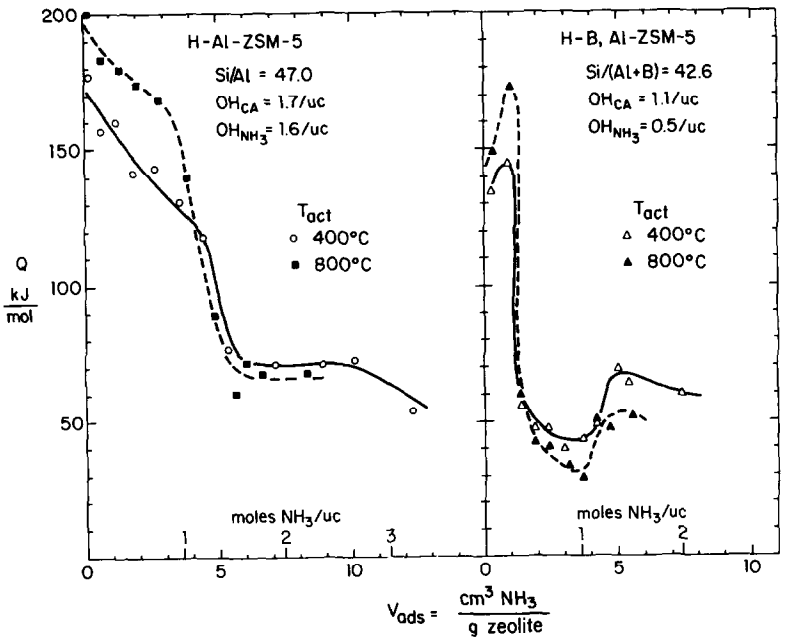

FIG. 4. Differential heats of ammonia adsorption on H–Al–ZSM-5 and H–B,Al–ZSM-5 at 148°C.

Similar shifts noted for other zeolites have been related to an increase in framework Al content (*51*).

Differences between B and Al pentasil zeolite spectra are best observed for self-supported wafers with respect to KBr pellets. New bands exist for the B samples at 1380, 970, 920, 700, and 670 cm^{-1}. The strongest band at 1380 cm^{-1} is 70 times weaker than that at 1100 cm^{-1} and is barely detectable in KBr pellets (Fig. 5).

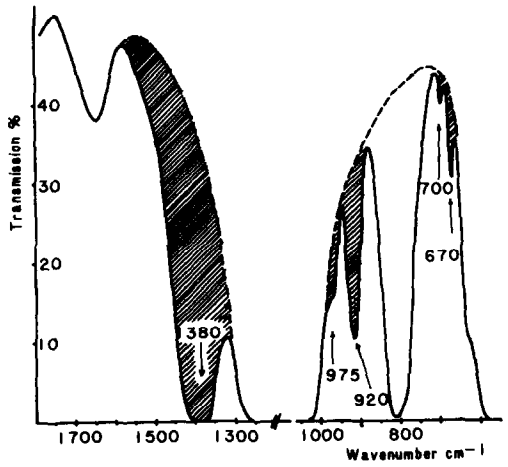

FIG. 5. Mid-infrared spectra of H–B–ZSM-11 evacuated at 400°C. Cross-hatched areas represent typical boralite bands.

These new bands, with the exception of the 970-cm^{-1} band, are related to the presence of boron and are observed in all boron pentasils (*52*) (Fig. 5). These assignments are based on comparison with IR spectra observed for binary borosilicate glasses (*53–57*) or films (*58–60*). In borates, a strong absorption in the region 1100–1400 cm^{-1} characterizes the B–O asymmetric stretching vibration of boron in three-fold coordination alone or in complex polymeric anions. In general higher frequencies reflect higher degrees of anion condensation (*60*, *61*). A high-frequency shift is also observed in B_2O_3 frameworks, when the B next-nearest neighbors are progressively replaced by less polarizing Si atoms. This results in an increase in the B–O bond order and consequently in a shift of the B–O asymmetric stretching frequency from 1265 to 1380 cm^{-1} (*53–58*).

The other absorptions at 920, 700, and

670 cm^{-1}, observed in all borosilicate glasses, are generally attributed to B–O–Si linkages (*53*, *54*). We assign these bands to the symmetric stretching vibration (920 cm^{-1}) and to the asymmetric and symmetric bending vibrations (700 and 670 cm^{-1}) of the BO_3 group in a symmetry lowered from D_{3h} to C_{3v}.

When ammonia, methanol, or to a lesser extent, water was adsorbed on the 400°C dehydrated boron zeolite samples, the intensities of the bands at 1380, 920, 700, and 670 cm^{-1} decreased to zero while a broad band near 1470 cm^{-1} developed (Fig. 6). This change was reversible since outgassing at room temperature totally restored the initial bands.

Such behavior was already mentioned by Taft (*59*) during hydration of borosilicate films and was interpreted as due to hydrolysis and formation of $B(OH)_3$ species. Scholle and Veeman (*16*) have studied boralite dehydration and rehydration using ^{11}B MAS NMR. They observed a change in the NMR spectrum which they interpreted as a transformation of trigonal boron to tetrahedral boron upon H_2O adsorption. Tetrahedral boron resulted in a narrow peak at 3 ppm similar to our site 1 NMR spectrum feature.

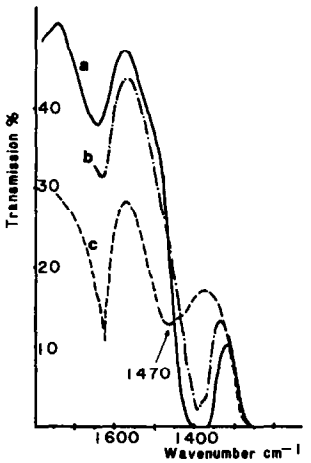

FIG. 6. Mid-infrared spectra of H–B–ZSM-11 showing effects of NH_3 adsorption. (a) After evacuation at 400°, (b) 0.5 Torr NH_3, (c) 35 Torr NH_3.

A triply degenerate BO_4 stretching mode is expected near 1096 cm^{-1} (*60*) and was indeed observed at 1130 and 926 cm^{-1} (degeneracy being removed) for danburite, a calcium borosilicate where B is tetrahedrally coordinated and at 1170 and 1090 cm^{-1} for BPO_4 (*62*, *63*). In the latter case, an excess of boron resulted in superficial BO_3 groups characterized by additional IR absorptions at 1400 and 710 cm^{-1} (*63*).

It is thus difficult to assign precisely the IR peaks to three- or four-coordination of B. It seems probable that because of the presence of intense SiO vibrations at 1100 cm^{-1}, BO_4 in T_d symmetry may not be detectable in boralite. Based on the changes in IR spectra upon NH_3, CH_3OH, or H_2O adsorption, we tentatively propose the following explanation. Due to its small size, boron is located near three oxygen atoms in a tetrahedral hole of the pentasil framework in a configuration similar to that described by Scholle and Veeman (*16*). This results in BO_3-type vibrational modes. Tetrahedral boron is obtained only by adding a fourth ligand giving site 1 as described in the NMR section.

b. Infrared spectra in the 1600- to 4000-cm^{-1} region. The spectra observed for the 400°C outgassed samples are shown in Fig. 7. They are composed of a narrow and intense peak at 3738 cm^{-1} with a shoulder at ca. 3700 cm^{-1} and a broad and intense peak at ca. 3520 cm^{-1}. The latter band was not detected for other boralite samples (*52*). It should be noted that when Al was not present (H–B–ZSM-11 sample), the 3610-cm^{-1} hydroxyl group band was not observed (Fig. 7). When Al impurity was present, a small peak at 3610 cm^{-1} was detected. We thus conclude that the 3610-cm^{-1} band is due to an acidic OH group related to lattice Al as suggested earlier (*64*).

After dehydroxylation at 800°C, all hydroxyl group bands disappeared, except a narrow band at 3745 cm^{-1} of low intensity with a small shoulder at 3730 cm^{-1}.

Upon adsorption of increasing incre-

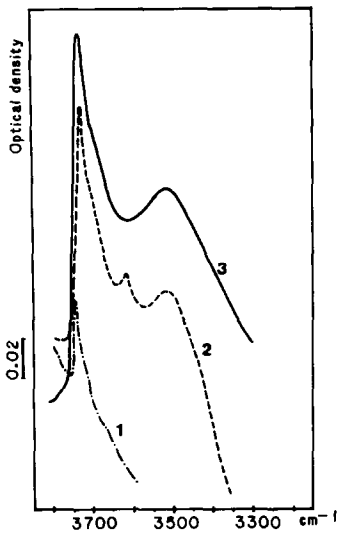

FIG. 7. Hydroxyl region of (1) H–B–ZSM-11 after evacuation at 400°C, (2) H–B,Al–ZSM-5 after evacuation at 400°C, (3) H–B,Al–ZSM-5 after evacuation at 800°C.

ments of NH_3, two bands at ca. 3385 and 3280 cm^{-1}, due to N–H stretching vibrations, developed progressively (Fig. 8). The intensities of the 3740- and 3520-cm^{-1} bands were observed to decrease only when the sample was equilibrated with a residual NH_3 pressure of the order of 0.1 Torr. This was totally reversible in the sense that both bands reappeared with their starting intensity upon outgassing at room temperature.

By analogy with IR spectra observed for borosilicate glasses, boron phosphate, and ZSM-5 zeolite, we suggest that the 3740- and 3700-cm^{-1} bands are due to terminal silanols (*64*) and to isolated B–OH groups (*63*, *65–68*). The 3520-cm^{-1} band which was perturbed only at appreciable NH_3 pressures may be assigned to gem OH groups ($B<^{OH}_{OH}$) or to internal OH groups as defined by Moffat and Neeleman (*67*).

The two absorption bands at ca. 3385 and 3290 cm^{-1} observed upon NH_3 adsorption may be assigned to B ← NH_3 species as in the case of Vycor glass (*66*), B_2O_3 on aerosil (*65*), and BPO_4 rich in B (*68*). They disappeared only after desorption at 150°C. The absence of other NH_3 or ammonium species stable under vacuum at room temperature allows us to conclude that the material has little or no Brønsted acidity in the usual meaning but weak Lewis acidity as shown by TPD and NMR (*69*). It is worth noting that ammonium borate does not exist since it is immediately decomposed into NH_3 and boric acid. In short, we tentatively suggest the following assignments.

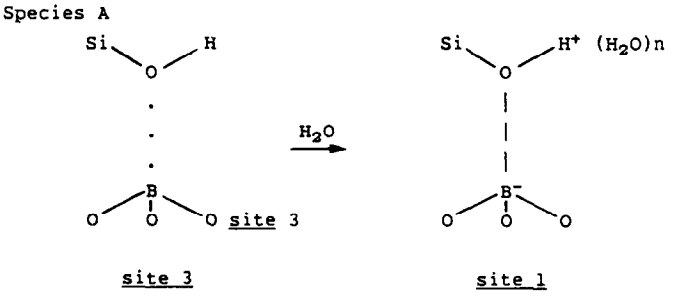

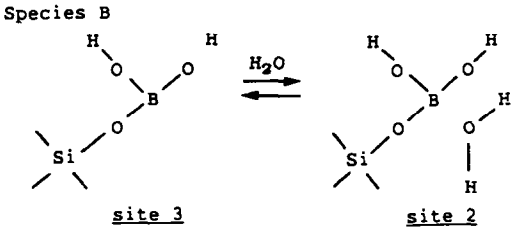

SPECIES A. A 3700-cm^{-1} band of weak acidity (*52*), detectable in IR for the sample outgassed at 400°C.

SPECIES B. The 3520-cm^{-1} groups which interact weakly and reversibly with NH_3 with H bonding of the type B–O–H...NH_3 and disappear irreversibly by calcining at 800°C.

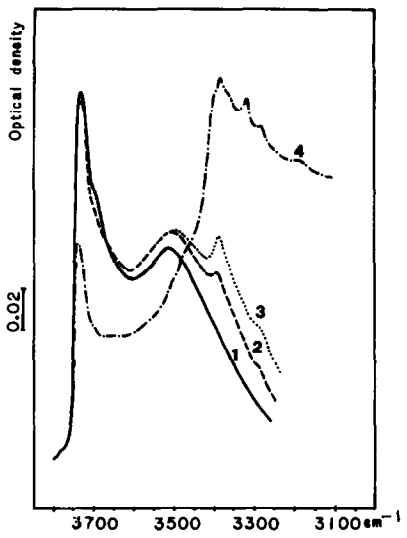

FIG. 8. Hydroxyl region after NH_3 adsorption on H–B–ZSM-11. (1) After evacuation at 400°C, (2) after adsorption of 0.28 NH_3/u.c., (3) 0.42 NH_3/u.c., (4) after equilibration with 0.5 Torr NH_3.

At NH_3 pressures >0.1 Torr formation of an ammonia complex probably occurs: we propose B–OH...$NH_3(NH_3)_4$ as suggested from microcalorimetry data.

E. Catalytic Results

When Al was not present in the zeolite (sample H–B–ZSM-11) no catalytic activity in methanol conversion and in toluene alkylation with methanol was observed. Only small amounts of dimethyl ether were detected. Increasing the CH_3OH reaction temperature up to 600°C results in the formation of appreciable amounts of light olefins but the lifetime is short.

For samples containing both Al and B the usual catalytic activity and selectivity characteristic of Al pentasils were obtained. It is striking to note that *para*-xylene selectivity in the toluene alkylation reaction was not enhanced in the presence of boron in contrast to boron-impregnated samples (*70*). The lifetime of the catalyst without regeneration was observed to increase with the amount of aluminum.

It may thus be concluded that boron at lattice sites in ZSM-5 and ZSM-11 zeolites does not introduce catalytic activity for the reactions studied, at least under usual conditions. This result is in agreement with the weak acidity resulting from the presence of lattice boron in contrast to aluminum as described above.

CONCLUSIONS

Boron introduced in the pentasil framework is four-coordinated when hydrated in two forms as evidenced by NMR (sites 1 and 2). Site 1 has already been reported previously (*16*). Site 2 corresponds to a new NMR spectrum tentatively assigned to a $H_2O(OH)_2B(OSi)$ species. By dehydration these two forms give rise to framework trigonal boron with B–OH and gem $B<^{OH}_{OH}$ groups exhibiting IR bands at 3700 and 3520 cm^{-1}, respectively, but exhibiting the same NMR spectrum (site 3).

The reversible transformation of four- to three-coordination upon dehydration is rather unusual for zeolite framework cations and may be related to the thermal instability of boron within the lattice (*70*).

The observation that site 2 is present in hydrated and partially hydrated samples suggests that all of the possible framework Si–O–B bridges are not formed in the materials studied. In ZSM-5, evidence for similar incomplete framework bridging is also available from ^{29}Si NMR (*71*), but dehydroxylation during calcination cures these framework defects.

In the literature, there are some discrepancies in the interpretation of three- or four-coordination from IR spectra. Interpretation of IR spectra is based on the assumption that small shifts result from changes in bond order, based solely on comparison with known standards. However, NMR spectra allow the coordination number about boron to be determined directly and unambiguously.

Both microcalorimetry and IR provide evidence that the presence of boron in the pentasil framework gives rise to only very weak acidity. This results in low catalytic

activity for acid-type reactions studied in methanol conversion and toluene alkylation with methanol.

ACKNOWLEDGMENTS

We thank C. M. Foris and R. L. Harlow for assistance in obtaining the X-ray data, H. Urbain and A. Chambosse for the Na and Al analyses, the Service Centrale d'Analyse du CNRS-Solaize for the B analyses, M. van Kavelaar for the scanning electron micrographs, and E. E. Carroll for the BET measurements. We are especially indebted to E. F. Moran for providing the samples of Na–ZSM-5 and Na–ZSM-11, and P. A. Jacobs of the Katholieke Universiteit of Leuven for providing a sample of ZSM-11. A. J. Vega derived expressions for the central transition lineshape during variable angle spinning. Computer programs written by M. K. Hanafey and L. C. Takiff were used in the analysis of the NMR spectra. Valuable discussions with D. R. Corbin are acknowledged. The spectra reported here were obtained with the assistance of R. F. Carver.

REFERENCES

1. Kokotailo, G. T., Lawton, S. L., Olson, D. H., and Meier, W. M., *Nature (London)* **275,** 437 (1978).
2. Kokotailo, G. T., Chu, P., Lawton, S. L., and Meier, W. M., *Nature (London)* **275,** 119 (1978).
3. (a) Weisz, P. B., *Pure Appl. Chem.* **52,** 2091 (1980); (b) Derouane, E. G., and Védrine, J. C., *J. Mol. Catal.* **8,** 479 (1980); (c) Derouane, E. G., *in* "Studies in Surf. Sci. and Catal. Series" (B. Imelik *et al.*, Eds.) Vol. 5, p. 5. Elsevier, Amsterdam, 1980; (d) Csicsery, S. M., *ACS Monogr.* **171,** 202 (1984).
4. Derouane, E. G., Dejaifve, P., B.Nagy, J. van Hooff, J. H. C., Spekman, B. P., Naccache, C., and Védrine, J. C., *C.R. Acad. Sci. Paris C* **285,** 945 (1977); *J. Catal.* **53,** 40 (1978).
5. Chen, N. Y., Kaeding, W. W., and Dwyer, F. G., *J. Amer. Chem. Soc.* **101,** 6783 (1979).
6. Kaeding, W. W., Chu, C., Young, L. B., and Butter, S. A., *J. Catal.* **69,** 392 (1981).
7. Klotz, M. R., Belgian Patent 859,656 (1978).
8. (a) Taramasso, M., Manara, G., Fattore, V., and Notari, B., French Patent 2.429,182 (1979); (b) Taramasso, M., Peredgo, G., and Notari, B., *in* "Proc. Vth Intern. Conf. on Molecular Sieves, Naples, 1980" (L. V. C. Rees, Ed.), p. 40. Heyden, London, 1980.
9. Holderich, W., Eichhorn, H., Lehnert, R., Marosi, L., Mross, W., Runke, R., Ruppel, W., and Schlimper, H., *in* "Proc. VIth Intern. Cong. on Molecular Sieves, Reno, 1983" (D. H. Olson and A Bisio, Eds.), p. 545. Butterworths, London, 1984.
10. Ione, K. G., Vostrikova, L. A., Paukshtis, E. A., Yurchenko, E. N., and Stepanov, V. G., *Dokl. Akad. Nauk, SSSR* **261,** 1160 (1981).
11. Vostrikova, L. A., Ione, K. G., Mastikhin, V. M., and Petrova, A. V., *React. Kinet. Catal. Lett.* **26,** 291 (1984).
12. Perego, G., Cesari, M., and Allegra, G., *J. Appl. Cryst.* **17,** 403 (1984).
13. Wengin, P., Guowen, L., Wangrong, L., and Bingxiong, L., "Intl. Symp. on Zeolites, Portorose, Yugoslavia, 1984."
14. Gabelica, Z., B.Nagy, J., Bodart, P., and Debras, G., *Chem. Lett.* **1984,** 1060 (1984).
15. Kutz, N. A., *in* "Proc. 2nd Symp. of Industry-University Coop. Chem. Prog., April 1–4, 1984," p. 120. Texas A&M Univ. Press, 1984.
16. Scholle, K. F. M. G. J., and Veeman, W. S., *Zeolites* **5,** 118 (1985).
17. Klotz, M. R., U.S. Patents 4,268,420; 4,269,813; 4,285,919 (1981).
18. Rollman, R. D., and Valyocsik, E. W., *Inorg. Synth.* **22,** 67 (1983).
19. Chu, P., U.S. Patent 3,709,979 (1973).
20. Taramasso, M., Manara, G., Fattore, V., and Notari, B., Ger. Patent 2,924,915 (1980).
21. Landolt, G. R., *Anal. Chem.* **42,** 613 (1971).
22. Gravelle, P. C., "Advances in Catalysis" (D. D. Eley, P. W. Selwood, and P. B. Weisz, Eds.), Vol. 22, p.191. Academic Press, New York, 1972.
23. Dominquez, J. M., Acosta, D. R., and Schifter, I., *J. Catal.* **83,** 480 (1983).
24. Haag, W. O., Lago, R. M., and Weisz, P. B., *Faraday Discuss. Chem. Soc.* **72,** 317 (1981).
25. von Ballmoos, R., "The O-Exchange Method in Zeolite Chemistry." Salle Sauerlander Verlag, Frankfurt, 1981.
26. Foger, K., Sanders, J. V., and Seddon, D., *Zeolites* **4,** 337 (1984).
27. Anderson, J. R., Foger, K., Mole, T., Rajadhyaksha, R. A., and Sanders, J. V., *J. Catal.* **58,** 114 (1979).
28. Shannon, R. D., *Acta. Crystallogr. A* **32,** 751 (1976).
29. Meyers, B. L., Ely, S. R., Kutz, N. A., Kaduk, J. A., and van den Bossche, E., *J. Catal,* **91,** 352 (1985).
30. Taylor, P. C., Baugher, J. F., and Kriz, H. M., *Chem. Rev.* **75,** 203 (1975).
31. Tzalmona, A., and Andrew, E. R., "Proc. 18th Ampère Conference, Nottingham," p. 241. North-Holland, Amsterdam, 1972.
32. Nolle, A., *Z. Phys. A* **280,** 231 (1977).
33. Vega, A. J., personal communication, 1981.
34. Kundla, E., Samosan, A., and Lippmaa, E., *Chem. Phys. Lett.* **83,** 229 (1981).
35. Fyfe, C. A., Gobbi, G. C., Hartman, J. S., Lenkinski, R. E., and O'Brien, J. H., *J. Magn. Reson.* **47,** 168 (1982); Meadows, M. D., Smith, K. A., Kinsey, R. A., Rothgeb, T. M., Skarjune, R. P.,

and Oldfield, E., *Proc. Natl. Acad. Sci. USA* **79,** 1351 (1982), and references therein.
36. Schramm, S., and Oldfield, E., *J. Chem. Soc. Chem. Commun.* **1982,** 980 (1982).
37. Jellison, G. E., Panek, L. W., Bray, P. J., and Rouse, G. B., *J. Chem. Phys.* **66,** 802 (1977).
38. Dell, W. J., Bray, P. J., and Xiao, S. Z., *J. Non-Cryst. Solids* **58,** 1 (1983); Bray, P. J., Geissberger, A. E., Bucholtz, F., and Harris, I. A., *J. Non-Cryst. Solids* **52,** 45 (1982).
39. Bray, P. J., Bucholtz, F., Geissberger, A. E., and Harris, I. A., *Nucl. Instrum. Methods* **199,** 1 (1982).
40. Turner, G. L., Smith, K. A., Kirkpatrick, R. James, and Oldfield, E., *J. Magn. Reson.* **67,** 544 (1986).
41. Gabelica, Z., Debras, G., and B.Nagy, J., *in* "Studies in Surf Sci. and Catal. Series" (S. Kaliaguine and A. Mahey, Eds.), Vol. 19, p. 113, 1984.
42. Vostrikova, L. A., Ione, K. G., Mastikhin, V. M., and Petrova, A. V., *React. Kinet. Catal. Lett.* **26,** 291 (1984).
43. Farlee, R. D., unpublished results.
44. Jellison, G. E., and Bray, P. J., *J. Non-Cryst. Solids* **29,** 187 (1978). (Site 2 in this paper has a B-10 quadrupole coupling constant of 1.5 MHz, corresponding to 0.72 MHz for B-11.)
45. Auroux, A., Védrine, J. C., and Gravelle, P. C., *in* "Studies in Surface Sci. and Catal. Series" (J. Rouquerol and K. S. W. Sing, Eds.), Vol. 10, p. 305. Elsevier, Amsterdam, 1982.
46. Auroux, A., Bolis, V., Wierzchowski, P., Gravelle, P. C., and Védrine, J. C., *J. Chem. Soc. Faraday Trans. 2* **75,** 2544 (1979).
47. Zhang, Y., *Inorg. Chem.* **21,** 3889 (1982).
48. Castleman, A. W., Holland, P. M., Lindsay, D. M., and Peterson, K. I., *J. Amer. Chem. Soc.* **100,** 6039 (1978).
49. Coudurier, G., Naccache, C., and Védrine, J. C., *J. Chem. Soc. Chem. Commun.*, 1413 (1982).
50. Jansen, J. C., van der Gaag, F. J., and van Bekkum, H., *Zeolites* **4,** 369 (1984).
51. Flanigen, E., *ACS Monogr.* **171,** 80 (1976).
52. Coudurier, G., and Védrine, J. C., *Pure Appl. Chem.* **58,** 1389 (1986).
53. Tenney, P. G., and Wong, J., *J. Chem. Phys.* **56,** 5516 (1972).
54. Jelliman, P. E., and Proctor, J. P., *J. Soc. Glass Technol.* **39,** 173T (1955).
55. Kumar, B., *Mater. Res. Bull.* **19,** 331 (1984).
56. Nogami, N., and Moriya, Y., *J. Non-Cryst. Solids* **48,** 359 (1982).
57. Kern, W., and Heim, R. C., *J. Electrochem. Soc.* **117,** 568 (1970).
58. Wong, J., *J. Electrochem Soc.* **127,** 62 (1980).
59. Taft, E. A., *J. Electrochem. Soc.* **118,** 1985 (1971).
60. Weir, C. E., and Schroeder, R. A., *J. Res. Nat. Bur. Stand. USA, Sect. A* **68** (1964).
61. Anderson, S., Bohrn, R. L., and Kimpton, D. D., *J. Amer. Ceram. Soc.* **38,** 370 (1955).
62. Osaka, A., Takahashi, K., and Ikeda, M., *J. Mater. Sci. Lett.* **3,** 36 (1984).
63. Haber, J., and Szybalska, U., *Faraday Discuss. Chem. Soc.* **72,** 263 (1981).
64. Védrine, J. C., Auroux, A., Bolis, V., Dejaifve, P., Naccache, C., Wierzchowski, P., Derouane, E. G., B.Nagy, J., Gilson, J. P., van Hooff, J. H. C., van den Berg, J. P., and Wolthuizen, J., *J. Catal.* **58,** 248 (1979).
65. Cant, N. W., and Little, L. H., *Canad. J. Chem.* **46,** 1373 (1968).
66. Low, M. J. D., and Subramanian, N. R., *J. Phys. Chem.* **70,** 2740 (1966).
67. Moffat, J. B., and Neeleman, J. F., *J. Catal.* **34,** 376 (1974).
68. Moffat, J. B., and Neeleman, J. F., *J. Catal.* **39,** 419 (1975).
69. Scholle, K. F. M. G. J., Kentgens, A. P. M., Veeman, W. S., Frenken, P., and van der Velden, G. P. M., *J. Phys. Chem.* **88,** 5 (1984).
70. Sayed, M., and Védrine, J. C., *J. Catal.* **101,** 43 (1986).
71. B.Nagy, J., Gabelica, Z., and Derouane, E. G., *Chem. Lett.* **1982,** 1105 (1982).